GEOPHYSICS, VOL. 71, NO. 4 (JULY-AUGUST 2006); P. SI103–SI110, 5 FIGS.
10.1190/1.2208967

A theoretical overview of model-based and correlation-based redatuming methods

Gerard T. Schuster[1] and Min Zhou[1]

ABSTRACT

We review the equations for correlation-based redatuming methods. A correlation-based redatuming method uses natural-phase information in the data to time shift the weighted traces so they appear to be generated by sources (or recorded by geophones) shifted to a new location. This compares to model-based redatuming, which effectively time shifts the traces using traveltimes computed from a prior velocity model. For wavefield redatuming, the daylight imaging, interferometric imaging, reverse-time acoustics (RTA), and virtual-source methods all require weighted correlation of the traces with one another, followed by summation over all sources (and sometimes receivers). These methods differ from one another by their choice of weights. The least-squares interferometry and virtual-source imaging methods are potentially the most powerful because they account for the limited source and receiver aperture of the recording geometry. Interferometry, on the other hand, has the flexibility to select imaging conditions that target almost any type of event. Stationary-phase principles lead to a Fermat-based redatuming method known as redatuming by a seminatural Green's function. No crosscorrelation is needed, so it is less expensive than the other methods. Finally, Fermat's principle can be used to redatum traveltimes.

INTRODUCTION

The oil industry has long used wave-equation redatuming of seismic data to remove elevation statics or to mitigate the defocusing effects of certain geologic bodies, such as the weathering zone or salt domes. Many workers have contributed to the wave-equation redatuming literature, including Berryhill (1979, 1986), Yilmaz and Lucas (1986), Bevc (1995), and Schneider et al. (1995). The idea is to apply time shifts to the data so the traces appear to be generated and recorded, respectively, by sources and receivers relocated to other places. These time shifts are effectively introduced by applying either Kirchhoff or wave-equation-based extrapolation operators to the data. For example, mountainous terrain with severe topography introduces severe elevation statics, so Kirchhoff extrapolation introduces time shifts that mitigate elevation-induced distortions in the data. The problem, however, is that the geologic velocity model must be known for wave-equation-based methods to work well. This is difficult in areas with severe statics problems that preclude effective velocity analysis.

Another type of redatuming is performed by applying time shifts explicitly to the traces to adjust for weathering-zone distortions (residual statics) or defocusing resulting from severe topography of the recording line (elevation statics). For residual statics (Rothman, 1986; Zhu et al., 1992; Marsden, 1993; Taner et al., 1998), the time shifts are estimated statistically from the data by crosscorrelating pilot traces with their neighboring traces. This compares to the wave-equation method that requires a velocity model to estimate the time shifts. The problem with residual statics is the sometimes implausible surface-consistency assumption, which says that rays near the free surface must be vertical. This means the time shifts do not truly honor the physics of wave propagation compared to wave-equation methods. A related redatuming method is the common-focus-point (CFP) method (Bolte and Verschuur, 2001; Kelamis et al., 2002), where traveltimes from the surface to a designated subsurface point are estimated from the shot gathers by focusing seismic sources iteratively toward a subsurface point while updating the involved traveltimes according to a semblance-based criterion.

Recently, redatuming methods based on crosscorrelation of seismic data have been developed to overcome the model-based limitations of wave-equation statics, the surface-consistency assumption of residual statics, or the need to strictly specify certain events in CFP technology. These new redatuming methods include reverse-time acoustics (RTA) (Fink, 1992; Blomgren et al., 2000; Lobkis and Weaver, 2001; Prada et al., 2002; Derode et al., 2003), daylight imaging (Rickett and Claerbout, 1996, 1999, 2000), interferometric body-wave imaging (Schuster and Rickett, 2000; Schuster, 2001; Sheng, 2001; Yu and Schuster, 2001, 2004; Schuster et al., 2004a; Zhou and Schuster, 2006), interferometric coda imaging (Snieder et

Manuscript received by the Editor April 8, 2005; revised manuscript received October 21, 2005; published online August 17, 2006.
[1]University of Utah, Department of Geology and Geophysics, Salt Lake City, Utah 84112. E-mail: schuster@mines.utah.edu; mzhou04@hotmail.com

al., 2002; Wapenaar et al., 2002; Snieder, 2004), and virtual-source imaging (Bakulin and Calvert, 2004; Calvert et al., 2004). Notable contributions to the theory of correlation-based imaging have been made by Wapenaar et al. (2002), Draganov et al. (2003), Wapenaar (2003, 2004), and Wapenaar et al. (2004). As will be shown, these methods all require weighted correlation of the traces with one another, followed by summation over all sources [and receivers for common-depth-point (CDP) datuming in Zhou and Schuster (2006)]. These methods differ from one another by their choice of weights and can be considered as special cases of the least-squares redatuming method described in this paper.

Key idea behind correlation

The key idea that underlies these correlation methods is that, in the frequency domain, two events are selected in the data: event

$$D(\mathbf{s}'|\mathbf{s}) = e^{i\omega(\tau^{\text{unint}}_{s's}+\tau^{\text{stat}})}$$

recorded at position $\mathbf{s}'$ and event

$$U(\mathbf{g}'|\mathbf{s}) = e^{i\omega(\tau^{\text{unint}}_{s's}+\tau^{\text{int}}_{g's'}+\tau^{\text{stat}})}$$

recorded at $\mathbf{g}'$. Here, the source statics time is represented by τ^{stat}, and the propagation traveltime in the uninteresting part of the medium from $\mathbf{x}'$ to $\mathbf{x}$ is denoted as $\tau^{\text{unint}}_{xx'}$. Figure 1 illustrates this idea, where $D(\mathbf{s}'|\mathbf{s})$ corresponds to the direct arrival measured along the drillstring while $U(\mathbf{g}'|\mathbf{s})$ corresponds to the upgoing reflected arrival measured at $\mathbf{g}'$. The direct wave and reflection events are similar in the sense that a portion of their raypaths coincides through uninteresting parts of the media (such as the overburden or weathering zone), so the correlated data $\phi(\mathbf{s}',\mathbf{g}',\mathbf{s})$=

$$D(\mathbf{s}'|\mathbf{s})^* U(\mathbf{g}'|\mathbf{s}) = e^{i\omega\tau^{\text{int}}_{g's'}}$$

retain the propagation information through the interesting portion of the medium and remove the uninteresting kinematic effects (i.e., eliminates $\tau^{\text{unint}}_{s's}$) as well as source statics for the source located at $\mathbf{s}$. Moreover, the correlated trace has the same traveltime $\tau^{\text{int}}_{g's'}$ as an event excited at $\mathbf{s}'$ and recorded at $\mathbf{g}'$, i.e., redatumed data. This partly overcomes the problems of model-based redatuming because the corrective time shifts come from the data.

In Figure 1, the location of the measured direct wave at $\mathbf{s}'$ fortuitously coincides with the intersection of the drillstring and the downgoing portion of the specular reflection ray. But how, in practice, do we know where to select $\mathbf{s}'$ so it coincides with the downgoing part of the specular reflection ray? Using stationary-phase theory, summation of the correlations $\phi(\mathbf{s}',\mathbf{g}',\mathbf{s})$ over all surface sources, i.e., $\Sigma_s\phi(\mathbf{s}',\mathbf{g}',\mathbf{s}) \approx e^{i\omega\tau^{\text{int}}_{g's'}}$, yields the dominant $e^{i\omega\tau^{\text{int}}_{g's'}}$ contribution at the stationary point $\mathbf{s} \rightarrow \mathbf{s}_o$ that coincides with the specular reflection ray. Thus, this summation automatically applies the correct time shifts to the specular arrivals at any incidence angle (Schuster and Rickett, 2000; Schuster et al., 2004a; Schuster et al., 2004b; Snieder, 2004) and so overcomes the implausible surface-consistency assumption.

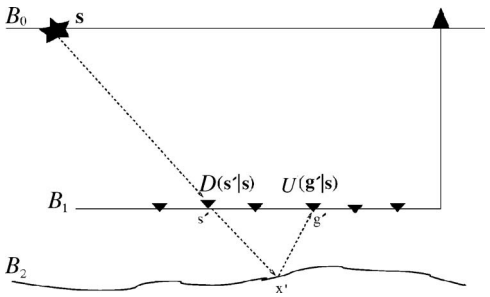

Figure 1. Deviated VSP geometry, where upgoing events $U(\mathbf{g}'|\mathbf{s})$ from below the drillstring and downgoing events $D(\mathbf{s}'|\mathbf{s})$ from above the drillstring are recorded. The primed letters $\mathbf{g}'$ and $\mathbf{s}'$ correspond to locations along the buried receiver string B_1, while the unprimed $\mathbf{s}$ corresponds to a surface source along B_0; the trial image point is denoted by $\mathbf{x}'$. The reflector geometry below the drillstring is represented by B_2.

The main part of this paper describes the theory for the correlation-based redatuming methods. The starting point is an integral forward-modeling equation followed by its approximation to the inverse. This inverse is an inner product of the weighted adjoint kernel with the data, so the methods are distinguished from one another by their choice of weighting terms. In addition, several new methods are introduced: redatuming by a seminatural Green's function (denoted as specular interferometry) and interferometric redatuming of traveltimes. The final section is a summary.

THEORY

Our goal is to derive the equations for redatuming correlated wavefields under a common mathematical framework. Toward this goal, we assume the 2D acoustic model in Figure 1 with the understanding that these methods can be generalized to the 3D elastic case. The sources on the surface and receivers at depth along a deviated vertical seismic profile (VSP) well are given in Figure 1. The well also can be oriented vertically as long as there are reflections from steeply dipping impedance boundaries such as faults or salt flanks. The velocity between the well and the surface is unknown, and the data will be used to image reflectors below or to one side of the buried receivers. The data $P(\mathbf{g}'|\mathbf{s})$ recorded at the well are defined as

$$P(\mathbf{g}'|\mathbf{s})|_{\mathbf{s}\epsilon B_0,\ \mathbf{g}'\epsilon B_1} = U(\mathbf{g}'|\mathbf{s}) + D(\mathbf{g}'|\mathbf{s}), \qquad (1)$$

where $U(\mathbf{g}'|\mathbf{s})$ and $D(\mathbf{g}'|\mathbf{s})$ correspond to the upgoing and downgoing waves in the frequency domain, respectively, recorded along the buried geophones for a surface source at $\mathbf{s}$. The primed letters $\mathbf{s}'$ and $\mathbf{g}'$ correspond to locations along the buried receiver string. All formulas are in the frequency domain, and we omit frequency notation for simplicity. Note the $D(\mathbf{g}'|\mathbf{s})$ and $U(\mathbf{g}'|\mathbf{s})$ fields are depicted as single-arrival events. More generally, they can represent multiple-arrival events so that the derivation below will be true for general wavefields with multiple angles of incidence.

Forward modeling

We will determine the forward-modeling equation for representing the scattered field along the buried geophones $\mathbf{g}'\epsilon B_1$ for a surface source along $\mathbf{s}\epsilon B_0$. According to a Huygens form of Green's theorem, the downgoing field $D(\mathbf{s}'|\mathbf{s})$ acts as a secondary source along the geophone string positions $\mathbf{s}'$ and reradiates to give a downgoing field at reflector positions $\mathbf{x}'$ along B_2, approximately represented by

$$D(\mathbf{x}'|\mathbf{s})|_{\mathbf{x}'\epsilon B_2} = \int_{B_1} \mathcal{G}(\mathbf{x}'|\mathbf{s}')D(\mathbf{s}'|\mathbf{s})ds', \qquad (2)$$

where the Green's function $\mathcal{G}(\mathbf{x}'|\mathbf{s}')$ satisfies the Helmholtz equation for a point source at $\mathbf{s}'$ and a buried geophone at $\mathbf{x}'$ in a medium with

a smooth velocity background. We can include more sophisticated weights, such as those for the Fresnel-Kirchhoff diffraction formula (Elmore and Heald, 1969; Wapenaar et al., 2005), but this simple form reduces notational clutter. For the remainder of this paper, we use Huygens's form of Green's theorem.

The downgoing field is incident on the reflector along B_2 to give rise to reflected upgoing waves $U(\mathbf{g}'|\mathbf{s})$ recorded at B_1. According to Huygens' form of Green's theorem, these upgoing fields can be represented by a weighted sum of the Green's functions, where the weight is the reflection coefficient:

$$U(\mathbf{g}'|\mathbf{s})\big|_{\mathbf{g}'\epsilon B_1,\ \mathbf{s}\epsilon B_0} = \int_{B_2} \mathcal{G}(\mathbf{g}'|\mathbf{x}')r(\mathbf{x}')D(\mathbf{x}'|\mathbf{s})dx'. \quad (3)$$

Here, the typical methods for separating up- and downgoing fields are used, such as f-k filtering or time windowing. The value $r(\mathbf{x}')$ represents the incident-angle-independent reflection coefficient for the interface along B_2, and $\mathbf{g}'$ is along B_1. Plugging equation 2 into equation 3 yields

$$U(\mathbf{g}'|\mathbf{s})\big|_{\mathbf{g}'\epsilon B_1,\mathbf{s}\epsilon B_0} = \int_{B_1} \Gamma(\mathbf{g}'|\mathbf{s}')D(\mathbf{s}'|\mathbf{s})ds', \quad (4)$$

where the reflection response given by $\Gamma(\mathbf{g}'|\mathbf{s}') = \int_{B_2}\mathcal{G}(\mathbf{g}'|\mathbf{x}')r(\mathbf{x}')\mathcal{G}(\mathbf{x}'|\mathbf{s}')dx'$ is interpreted as the redatumed shot gather for $\mathbf{s}'$, $\mathbf{g}'\epsilon B_1$. Equation 4 represents the forward-modeling equation used to compute a shot gather for a surface source and scattered energy recorded along the buried geophone string at B_1. The scattering occurs exclusively along the B_2 interface. The following section shows how to invert this equation to get $\Gamma(\mathbf{g}'|\mathbf{s}')$ for $\mathbf{g}',\mathbf{s}'\epsilon B_1$.

Inverse modeling

Claerbout (1992) reiterates the idea that the inverse to the forward-modeling problem expressed by equation 4 can be approximated by taking the inner product of the adjoint kernel $D(\mathbf{s}'|\mathbf{s})^*$ with the data $U(\mathbf{g}'|\mathbf{s})$ to get an estimate of the model, which in our case is the reflection response $\Gamma(\mathbf{g}'|\mathbf{s}')$. Therefore,

$$\Gamma(\mathbf{g}'|\mathbf{s}')\big|_{\mathbf{g}',\mathbf{s}'\epsilon B_1} \approx \int_{B_0} D(\mathbf{s}'|\mathbf{s})^* U(\mathbf{g}'|\mathbf{s})ds, \quad (5)$$

where $\Gamma(\mathbf{g}'|\mathbf{s}')$ is the redatumed shot gather and the integration is over the surface sources along B_0. The product $D(\mathbf{s}'|\mathbf{s})^*U(\mathbf{g}'|\mathbf{s})$ represents correlations of upgoing and downgoing traces in the time domain; their summation over sources only forms an approximate inverse because practical source distributions never continuously surround the target body as required by theory (Wapenaar, 2004).

A more accurate inverse that accounts for the limited source-receiver aperture and discrete source and receiver sampling can be obtained by recognizing that equation 4, after substituting in the asymptotic Green's function at high frequencies, is similar to the generalized Radon transform (GRT) given in Beylkin (1985). Thus, the asymptotic inverse can be estimated by an inner product of the data with the weighted adjoint (Bleistein et al., 2001):

$$\Gamma(\mathbf{g}'|\mathbf{s}')\big|_{\mathbf{g}',\mathbf{s}'\epsilon B_1} = \int_{B_1}\int_{B_0} \kappa(\mathbf{s}'|\mathbf{s}''|\mathbf{s})D(\mathbf{s}''|\mathbf{s})^* U(\mathbf{g}'|\mathbf{s})ds ds'' \quad (6)$$

$$\approx \int_{B_0} k(\mathbf{s}'|\mathbf{s})D(\mathbf{s}'|\mathbf{s})^* U(\mathbf{g}'|\mathbf{s})ds, \quad (7)$$

where $\kappa(\mathbf{s}'|\mathbf{s}''|\mathbf{s})$ is the asymptotic inverse kernel and $k(\mathbf{s}'|\mathbf{s})$ is a preconditioning kernel. For example, $\kappa(\mathbf{s}'|\mathbf{s}''|\mathbf{s}) = k(\mathbf{s}'|\mathbf{s})\delta(\mathbf{s}'' - \mathbf{s}')$ inserted into equation 6 yields equation 7.

Different approximations to the kernel $k(\mathbf{s}'|\mathbf{s})$ lead to various forms of redatuming algorithms:

$$k(\mathbf{s}'|\mathbf{s}) \approx \begin{cases} 1 & \text{Daylight and RTA redatuming} \\ \dfrac{\mathcal{M}(\omega,\mathbf{s},\mathbf{s}')\star}{|W(\omega)|^2 + \epsilon} & \text{Interferometric redatuming} \\ \dfrac{\mathcal{W}(\omega)}{\int_{B_0} |D(\mathbf{s}'|\mathbf{s}_o)|^2 ds_o + \epsilon} & \text{Virtual-source redatuming} \\ \dfrac{G(\mathbf{s}'|\mathbf{s})^*}{D(\mathbf{s}'|\mathbf{s})^*} & \text{Kirchhoff redatuming} \\ \dfrac{\delta(\mathbf{s} - \mathbf{s}_o)e^{i\omega\tilde{\tau}_{ss'}}}{D(\mathbf{s}'|\mathbf{s})^*} & \text{Specular interferometric redatuming} \\ [\mathbf{D}^*\mathbf{D}]^{-1} & \text{Least-squares redatuming} \end{cases} \quad (8)$$

Here, $\mathbf{s}_o$ is the specular source point that excites a specular ray that passes through $\mathbf{s}'$ and $\mathbf{g}'$, $W(\omega)$ represents the actual source spectrum, and $\mathcal{W}(\omega)$ represents the desired source spectrum. The value $\mathcal{M}(\omega,\mathbf{s},\mathbf{s}')\star$ represents the frequency-domain convolution of the spectrum associated with a muting function in the time domain; this function zeros out all but the arrivals of interest in the space-time traces, such as ringy direct arrivals for VSP data (Yu and Schuster, 2004) or a reference reflection (Zhou and Schuster, 2006) for CDP data. In some cases no muting is needed because correlation of unmuted VSP traces can produce high-quality images of salt flanks from diving waves (Hornby et al., 2006). The following subsections explain the meaning of each kernel.

Daylight and RTA redatuming

The daylight redatuming kernel in equation 8 is used for the daylight imaging algorithm developed by Claerbout and his students in the 1990s (Rickett and Claerbout, 1996, 1999, 2000). They proposed that seismic data generated by a random distribution of buried sources and measured on the free surface can be transformed naturally (i.e., redatumed) to traces generated by virtual surface sources. The key idea is that the upcoming waves $U(\mathbf{s}'|\mathbf{s})^{\text{direct}}$ from buried sources at $\mathbf{s}$ strike the earth's free surface at $\mathbf{s}'$ and reradiate downward, as if each point $\mathbf{s}'$ on the free surface acts as a secondary source. (Daylight data should be preprocessed to separate the data into the appropriate up- and downgoing components in order to use equation 8.) This is illustrated in Figure 2, which is identical to Figure 1 except the surface source in Figure 1 has been mirrored across B_1, and B_1 is now a free surface. These secondary sources at $\mathbf{s}'$ excite a new family of upgoing reflections $U(\mathbf{g}'|\mathbf{s})^{\text{ghost}}$ measured at $\mathbf{g}'$ on the free surface. The start time of these recorded ghost reflections is advanced to their excitation time at the free surface by crosscorrelating (multiplying the conjugated trace by another trace in the frequency domain) the recorded source arrivals $U(\mathbf{s}'|\mathbf{s})^{\text{direct}}$ with the ghosts. These correlated

data are then summed over all surface source positions:

$$\Gamma(\mathbf{g}'|\mathbf{s}') \approx \int_{B_0} U(\mathbf{g}'|\mathbf{s})^{\text{ghost}} U(\mathbf{s}'|\mathbf{s})^{\text{direct}*} ds, \qquad (9)$$

where the approximation is used to reflect the fact that practical receiver distributions on the surface are limited in aperture. The summation over the randomly distributed sources is needed to achieve diversity of incident source rays at $\mathbf{s}'$, which can excite diverse specular reflections for a secondary source at $\mathbf{s}'$ and receiver at $\mathbf{g}'$. Note in equation 9 that we replace $U(\mathbf{g}'|\mathbf{s})^{\text{ghost}} \rightarrow U(\mathbf{g}'|\mathbf{s})$, $U(\mathbf{s}'|\mathbf{s})^{\text{direct}*} \rightarrow D(\mathbf{s}'|\mathbf{s})^*$, and $k(\mathbf{s}'|\mathbf{s}) = 1$ to get equation 5. If pressure geophones are used rather than vertical velocity geophones, then a reflection coefficient of -1 should be taken into account.

The RTA redatuming kernel is identical to the daylight imaging kernel. However, the RTA literature usually describes redatuming as how the Green's function can be "recovered by summing the cross-correlations" (Derode et al., 2003) of the traces at $\mathbf{s}'$ and $\mathbf{g}'$ to get $\Gamma(\mathbf{g}'|\mathbf{s}')$. This Green's function is the same as data redatumed for a source at $\mathbf{s}'$ and a receiver at $\mathbf{g}'$ (Draganov et al., 2003; Wapenaar, 2003, 2004).

Interferometric redatuming

The interferometric redatuming kernel can be found lurking in the interferometric imaging equations presented by Schuster and Rickett (2000), Schuster (2001), Sheng (2001), Yu and Schuster (2001), Schuster et al. (2004a), and Schuster et al. (2004b). (Interferometric imaging is sometimes known as crosscorrelation migration.) For the reverse VSP model in Figure 2, the interferometric imaging equation for migrating ghost reflections is given by

$$\begin{aligned} m(\mathbf{x}') &= \int_{s'\epsilon B_1}\int_{g'\epsilon B_1}\int_{s\epsilon B_0} \frac{U(\mathbf{g}'|\mathbf{s})^{\text{ghost}} U(\mathbf{s}'|\mathbf{s})^{\text{direct}*}}{|W(\omega)|^2+\epsilon} \\ &\quad \times e^{-i\omega(\tau_{g'x'}+\tau_{x's'})} ds dg' ds', \\ &= \int_{s'\epsilon B_1}\int_{g'\epsilon B_1} \Gamma(\mathbf{g}'|\mathbf{s}') e^{-i\omega(\tau_{g'x'}+\tau_{x's'})} dg' ds', \end{aligned} \qquad (10)$$

where $m(\mathbf{x}')$ is the migration image at the trial image point $\mathbf{x}'$,

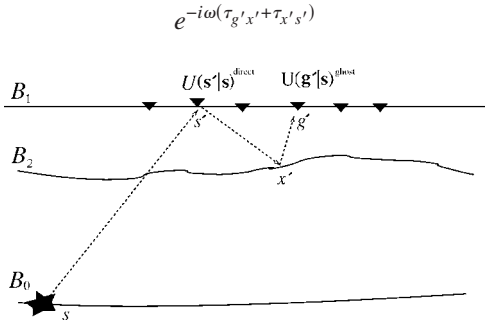

Figure 2. Each point on the free surface acts as a secondary source of seismic energy so that the direct arrivals $U^{\text{direct}}(\mathbf{s}'|\mathbf{s})$ from a buried source $\mathbf{s}$ into the ghost reflections $U^{\text{ghost}}(\mathbf{g}'|\mathbf{s})$. This picture is obtained by mirroring the source rays in Figure 1 across the receiver string and replacing B_1 by a free surface. Here, B_0 does not need be a physical boundary.

is the migration kernel, τ_{ab} represents the traveltime for waves to propagate from $\mathbf{a}$ to $\mathbf{b}$, $U(\mathbf{s}'|\mathbf{s})^{\text{direct}*} = \mathcal{M}(\omega,\mathbf{s},\mathbf{s}') \star U(\mathbf{s}'|\mathbf{s})^*$ is the windowed direct wave or other arrivals of interest that generate the upgoing ghost arrivals, $1/(|W(\omega)|^2+\epsilon)$ is the inverse filter for the correlated source-wavelet deconvolution, and the redatumed data are given by

$$\Gamma(\mathbf{g}'|\mathbf{s}') = \int_{s\epsilon B_0} \frac{U(\mathbf{g}'|\mathbf{s})^{\text{ghost}} U(\mathbf{s}'|\mathbf{s})^{\text{direct}*}}{|W(\omega)|^2+\epsilon} ds. \qquad (11)$$

This redatuming equation is the same as that for daylight imaging in equation 9, except the correlated source wavelet is deconvolved by the deconvolution filter $1/(|W(\omega)|^2+\epsilon)$ and the muting function is used to select certain events. There are many variants of body-wave interferometric imaging in exploration geophysics, including CDP multiple imaging (Sheng, 2001), CDP primary redatuming (Zhou and Schuster, 2006), P-to-S (PS) transmission imaging (Schuster et al., 2004b; Xiao et al., 2006), salt flank imaging by VSP primary reflections (Hornby et al., 2006), and higher-order VSP multiple imaging (Schuster, 2003; Jiang et al., 2005). As an example for a deviated VSP geometry, the correlation equation given by

$$\Gamma(\mathbf{g}'|\mathbf{s}') = \int_{s\epsilon B_0} \frac{U(\mathbf{g}'|\mathbf{s})^{\text{refl}} D(\mathbf{s}'|\mathbf{s})^{\text{direct}*}}{|W(\omega)|^2+\epsilon} ds \qquad (12)$$

applies to the source-receiver geometry in Figure 1 so that the sources are redatumed to the level of the buried drillstring.

Virtual-source imaging

Virtual-source imaging was introduced by Bakulin and Calvert (2004) and Calvert et al. (2004) in the context of the deviated-well VSP example in Figure 1. Here, the sources are on the surface and the receivers are along the buried well string. The correlation equation is similar to equation 12, except

$$\frac{D(\mathbf{s}'|\mathbf{s})^{\text{direct}*}}{|W(\omega)|^2+\epsilon}$$

is replaced by a preconditioning term such as

$$\frac{\mathcal{W}(\omega) D(\mathbf{s}'|\mathbf{s})^*}{\int_{B_0} |D(\mathbf{s}'|\mathbf{s}_o)|^2 ds_o + \epsilon},$$

with the recognition that the entire downgoing field $D(\mathbf{s}'|\mathbf{s})$ is the generalized source wavelet for the upgoing field. In this case, the redatuming equation becomes

$$\Gamma(\mathbf{g}'|\mathbf{s}') = \int_{s\epsilon B_0} \frac{\mathcal{W}(\omega) U(\mathbf{g}'|\mathbf{s})^{\text{refl}} D(\mathbf{s}'|\mathbf{s})^*}{\int_{B_0} |D(\mathbf{s}'|\mathbf{s}_o)|^2 ds_o + \epsilon} ds. \qquad (13)$$

A preconditioning kernel approximates the actual inverse kernel and is designed to convert downgoing wave records at the receiver string in Figure 1 into pulses at zero time. Here, the time-reversed wavefield for $D(\mathbf{s}'|\mathbf{s})$ will phase deconvolve the physical source and source-to-well transmission response to zero phase at time zero. The term $\mathcal{W}(\omega)$ is the desired pulse wavelet taken to have the highest common bandwidth of $D(\mathbf{g}'|\mathbf{s})$, and $1/(\int_{B_0}|D(\mathbf{s}'|\mathbf{s}_o)|^2 ds_o + \epsilon)$ gives a stabilized amplitude deconvolution.

Use equation 13 to collect all of the energy arriving upward at $\mathbf{g}'$ that also has passed through $\mathbf{s}'$ and been converted to a pulse. Thus, provided the physical source has illuminated $\mathbf{s}'$ with downgoing waves that are scattered back to $\mathbf{g}'$, we have a way of imaging this energy as though we had a virtual source with known pulse $\mathcal{W}(\omega)$ at $\mathbf{s}'$. Surprisingly, perhaps, greater overburden complexity and longer reverberations suggest that using longer time windows in the traces for imaging will lead to better resolution and less need for dense source sampling. The actual equation and implementation of virtual-source imaging is slightly different than that for equation 13.

In comparison to interferometric redatuming, Schuster et al. (2004b) and Yu and Schuster (2004) perform both natural extrapolation and migration using mostly single-arrival Kirchhoff integrals, while Calvert et al. (2004) and Bakulin and Calvert (2004) use natural extrapolation with multiarrival Kirchhoff integrals. The theoretical benefit is that multiarrival Kirchhoff integrals have the potential for superresolution, accounting for a wide diversity of reflection arrivals.

Kirchhoff redatuming

Most conventional datuming techniques (Berryhill, 1979, 1986; Yilmaz and Lucas, 1986; Bevc, 1995; Schneider et al., 1995) require detailed knowledge of the velocity model above the datum horizon. Thus, a good estimate of the velocity model must be known to extrapolate data accurately from the measuring plane to another depth level. Typically, both shots and receivers are extrapolated. Inserting the kernel $k(\mathbf{s}'|\mathbf{s}) = G(\mathbf{s}'|\mathbf{s})^*/D(\mathbf{s}'|\mathbf{s})^*$ into equation 7 yields the source extrapolation (i.e., redatuming) operator for either the Figure 1 or the Figure 2 example. This differs from the correlation-based redatuming methods in that the redatuming kernel is not natural because the Green's function $G(\mathbf{s}'|\mathbf{s})$ must be computed from an a priori velocity model. In practice, a more accurate dipole (rather than a monopole) extrapolation kernel is sometimes used (Bevc, 1995).

Specular interferometric redatuming

If the kernel in equation 7 is replaced by $k(\mathbf{s}'|\mathbf{s}) = \delta(\mathbf{s} - \mathbf{s}_o)\, e^{-i\omega\tilde{\tau}_{s's}}/D(\mathbf{s}'|\mathbf{s})^*$, then

$$\Gamma(\mathbf{g}'|\mathbf{s}')\big|_{\mathbf{g}',\mathbf{s}'\epsilon B_1} = \int_{B_0} \delta(\mathbf{s} - \mathbf{s}_o) e^{-i\omega\tilde{\tau}_{s's}} U(\mathbf{g}'|\mathbf{s})\, ds$$
$$= e^{-i\omega\tilde{\tau}_{s's_o}} U(\mathbf{g}'|\mathbf{s}_o), \qquad (14)$$

where $\mathbf{s}_o$ is the special source position on the surface such that a specular transmitted ray intersects both the given values of $\mathbf{s}'$ and a given trial image point $\mathbf{x}'$, as depicted in Figure 3. In this case of a deviated VSP geometry, $\mathbf{s}_o$ is a function of the specified points $\mathbf{s}'$ and $\mathbf{x}'$.

Therefore, equation 14 says that the trace at $\mathbf{g}'$ is advanced in time by exactly the traveltime for specular energy to go from the surface at $\mathbf{s}_o$ to the drillstring point at $\mathbf{s}'$. This is denoted as redatuming by a seminatural Green's function (Schuster, 2003) or sometimes as specular interferometric redatuming. Here, $\tilde{\tau}_{s's_o}$ is the picked traveltime of the direct wave for propagating from the surface source location at $\mathbf{s}_o$ to the specified wellstring position $\mathbf{s}'$. This traveltime can be found by using Fermat's principle to find $\mathbf{s}_o$ for a given $\mathbf{s}'$ and trial image point $\mathbf{x}'$:

$$\mathbf{s}_o = \{\mathbf{s}|\min_{\mathbf{s}\epsilon B_0}(\tau_{x's'} + \tilde{\tau}_{s's})\}. \qquad (15)$$

Once $\mathbf{s}_o$ is identified, then $\tilde{\tau}_{s's_o}$ is the direct wave traveltime picked from the data (see Figure 3b). Note the $\tau_{x's'}$ in the minimization brackets is computed by ray tracing from the model.

The above kernel is used by Schuster (2003) and Zhou and Schuster (2006) for CDP interferometric imaging, and related kernels are used by Jiang et al. (2005; personal communication, 2005) for VSP interferometric imaging. The advantage is a reduction of migration artifacts and computational time compared to standard interferometric imaging.

Least-squares redatuming

A convenient form for the inverse of equation 4 is obtained by representing its discrete form in matrix-vector notation:

$$\mathbf{u} = \mathbf{D}\gamma, \qquad (16)$$

where $U \rightarrow \mathbf{u}$ and $\Gamma \rightarrow \gamma$ are $M \times 1$ and $N \times 1$ vectors, respectively, and $D \rightarrow \mathbf{D}$ is an $M \times N$ matrix. The least-squares estimate of the reflection response function $\Gamma(\mathbf{g}'|\mathbf{s}')$ is then given by solving the normal equations

$$[\mathbf{D^T D}]\gamma = \mathbf{D^T u} \qquad (17)$$

to get

$$\gamma = [\mathbf{D^T D}]^{-1}\mathbf{D^T u}, \qquad (18)$$

where the Hessian inverse is given by $[\mathbf{D^T D}]^{-1}$ and $\mathbf{D}^T$ is the adjoint of the forward-modeling operator in equation 4. Formally, $[\mathbf{D^T D}]_{s''s'} = \int_{B_0} D(\mathbf{s}''|\mathbf{s})^* D(\mathbf{s}'|\mathbf{s})\, ds$. If the sources are distributed densely around the target and have uncorrelated phases, then the summation of terms in this integrand for $\mathbf{s}' \neq \mathbf{s}''$ will, on average, cancel. Thus, the inverse Hessian can be approximated roughly in the far field as the preconditioning term $[\mathbf{D^T D}]^{-1}_{s''s'} \approx 1/[\mathbf{D^T D}]_{s''s'} \times \delta(\mathbf{s}' - \mathbf{s}'')$, which is a variant of the virtual-source deconvolution filter.

The least-squares solution requires the inverse Hessian $[\mathbf{D^T D}]^{-1}$ operator, so the $k(\mathbf{s}'|\mathbf{s})$ symbol for least-squares redatuming in equa-

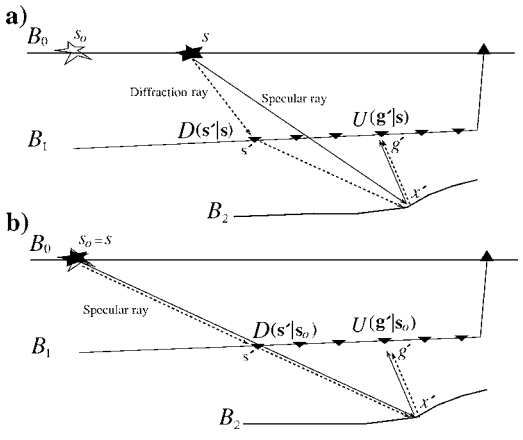

Figure 3. For fixed $\mathbf{s}'$ along the receiver string B_1 and $\mathbf{x}'$ trial image positions, the traveltime difference between the solid specular and dashed diffraction rays is minimized when the solid star at $\mathbf{s}$ coincides with the open star at $\mathbf{s}_o$. This traveltime difference is nonzero in (a) but zero in (b). The reflections can emanate from a steeply dipping impedance boundary such as a fault or salt flank.

tion 8 represents the operator $\int_{B_1} ds'' \kappa(\mathbf{s}'|\mathbf{s}'')|\mathbf{s}_o)$ seen in equation 6. Other approximate inverses can be used, such as adaptive successive overrelaxation, block Jacobi methods, generalized conjugate gradients (Hageman and Young, 1981) or Beylkin's asymptotic inverse. In principle the least-squares inverse should provide the most effective datuming for limited-aperture data with discrete sampling of sources and receivers.

Traveltime redatuming

Consider Figure 4, which depicts the transform of VSP data from two nearby wells to virtual crosswell data. Such data can be used to produce high-resolution tomograms or reflectivity images where the sources and receivers are along the well rather than the surface. Here, $U(\mathbf{g}'|\mathbf{s})$ in equation 7 represents the reflected arrival recorded by receivers in the well farthest from the source (right well), while $D(\mathbf{s}'|\mathbf{s})$ represents the direct arrivals recorded in the well closest to the surface (left well). Multiplying $U(\mathbf{g}'|\mathbf{s})$ with $D(\mathbf{s}'|\mathbf{s})^*$ and summing over all $\mathbf{s}$ at the surface yields the redatumed shot gather $\Gamma(\mathbf{g}'|\mathbf{s}')|_{\mathbf{s}'\epsilon B_1,\mathbf{g}'\epsilon B_2}$ for sources in the left well and receivers in the right well. The redatumed shot gather can be migrated to give the reflectivity image. The velocity model of the salt and layers above are not needed because the VSP data are transformed to be apparent crosswell data with virtual sources and receivers in the well. Transmission traveltime tomography can be performed on these data by using the redatumed direct arrivals in the left and right wells.

Instead of redatuming wavefields by Green's theorem, we can redatum traveltimes by Fermat's principle. According to Fermat's principle, the redatumed traveltimes (Schuster, 2005a, b) can be found by picking the direct-wave traveltimes along each well and calculating their minimum difference:

$$\tilde{\tau}^{\text{direct}}_{s'g'}|_{\mathbf{s}'\epsilon B_1,\mathbf{g}'\epsilon B_2} = \min_{\mathbf{s}\epsilon B_0}(\tilde{\tau}^{\text{direct}}_{g's} - \tilde{\tau}^{\text{direct}}_{s's}), \qquad (19)$$

where the tildes denote picked direct-wave traveltimes in the VSP data. Here, $\tilde{\tau}_{s'g'}$ is the redatumed direct-wave traveltime for a source at $\mathbf{s}'$ in the left well and $\mathbf{g}'$ is a receiver in the right well.

Similarly, the redatumed reflection traveltimes are computed by using a slightly different version of Fermat's principle:

$$\tilde{\tau}^{\text{refl}}_{s'g'}|_{\mathbf{s}'\epsilon B_1,\mathbf{g}'\epsilon B_2} = \min_{\mathbf{s}\epsilon B_0}(\tilde{\tau}^{\text{refl}}_{g's} - \tilde{\tau}^{\text{direct}}_{s's}), \qquad (20)$$

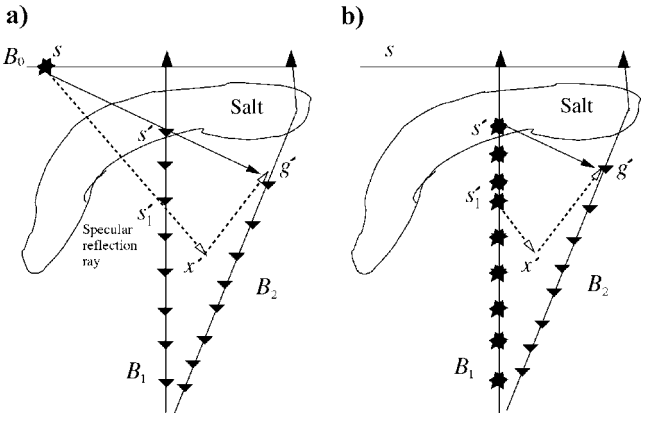

Figure 4. (a) VSP shot gathers recorded along the two wells can be transformed into (b) an apparent crosswell data set after interferometric correction (for wavefields) or Fermat correction (for traveltimes).

where $\tilde{\tau}^{\text{refl}}_{g's}$ is the picked traveltime of the reflections in the right well. Fermat's principles have been used for a wide variety of tasks, including the prediction of traveltimes for multiples from primary traveltimes (Asakawa and Matsuoka, 2002; Reshef et al., 2003).

WHY CORRELOGRAM SUMMING EQUALS EXTRAPOLATION

Why does the summation over the VSP correlograms in equation 5 produce correlograms excited by virtual sources buried at $\mathbf{s}'$ rather than sources at the surface? The answer can be found by examining the single scatterer model in Figure 3a. Here, the downgoing and upcoming data are given by

$$D(\mathbf{s}'|\mathbf{s}) = e^{i\omega\tilde{\tau}_{s's}};\ U(\mathbf{g}'|\mathbf{s}) = e^{i\omega\tilde{\tau}^{\text{refl}}_{g'x's}}, \qquad (21)$$

where geometric spreading and reflection effects are ignored, $\tilde{\tau}^{\text{refl}}_{g'x's}$ is the traveltime associated with the solid specular reflection ray in Figure 3a, and $\tilde{\tau}_{s's}$ is the traveltime for the direct arrival denoted by the dashed ray.

Plugging equation 21 into equation 5 yields

$$\begin{aligned}\Gamma(\mathbf{g}'|\mathbf{s}') &= \int e^{i\omega(\tilde{\tau}^{\text{refl}}_{g'x's} - \tilde{\tau}_{s's})} ds, \\ &= e^{i\omega(\tilde{\tau}_{g'x'} + \tilde{\tau}_{x's'})} \int e^{-i\omega(\overbrace{\tilde{\tau}_{g'x'} + \tilde{\tau}_{x's'} + \tilde{\tau}_{ss'}}^{\text{diffraction}} - \overbrace{\tilde{\tau}^{\text{refl}}_{g'x's}}^{\text{specular}})} ds,\end{aligned} \qquad (22)$$

where $i\omega(\tilde{\tau}_{g'x'} + \tilde{\tau}_{x's'})$ is added and subtracted in the exponential argument. The specular reflection traveltime $\tau^{\text{refl}}_{g'x's}$ is always less than the diffraction time (in a small neighborhood around the specular reflection point) in Figure 3a, unless the surface source location at $\mathbf{s}$ coincides with the open star at $\mathbf{s}_o$ in Figure 3b. In this case, the phase of the integrand's exponential is zero because the diffraction and specular reflection traveltimes are equal. This source location $\mathbf{s} \to \mathbf{s}_o$, according to stationary-phase theory, makes the maximum contribution to the integral. Thus, equation 22 asymptotically becomes

$$\Gamma(\mathbf{g}'|\mathbf{s}') \sim Ce^{i\omega(\tilde{\tau}_{g'x'} + \tilde{\tau}_{x's'})}, \qquad (23)$$

where C is the asymptotic constant. Except for the constant C, $\Gamma(\mathbf{g}'|\mathbf{s}')$ enjoys the kinematics of a reflection arrival for a source buried at $\mathbf{s}'$ and a buried receiver at $\mathbf{g}'$ with a specular reflection at $\mathbf{x}'$. This is the definition of data kinematically redatumed such that the field resulting from a surface source has been extrapolated to the buried drillstring.

Transforming pegleg multiples into primaries

What about events such as pegleg multiples generated at the surface to become downgoing events recorded along the receiver string (see Figure 5a)? In this case there will be a downgoing pegleg multiple

$$D(\mathbf{s}'|\mathbf{s})|_{\mathbf{s}\epsilon B_0;\mathbf{s}'\epsilon B_1} = e^{i\omega\tau^{\text{peg}}_{s's}} \qquad (24)$$

that will generate an upgoing pegleg multiple reflection denoted as

$$U(\mathbf{g}'|\mathbf{s})|_{\mathbf{s}\epsilon B_0;\mathbf{g}'\epsilon B_1} = e^{i\omega\tau^{\text{peg}}_{g'x's}}, \qquad (25)$$

where $\tau_{g'x's}$ is the specular pegleg reflection recorded at $\mathbf{g}'$ shown in Figure 5a. The correlated data are given by

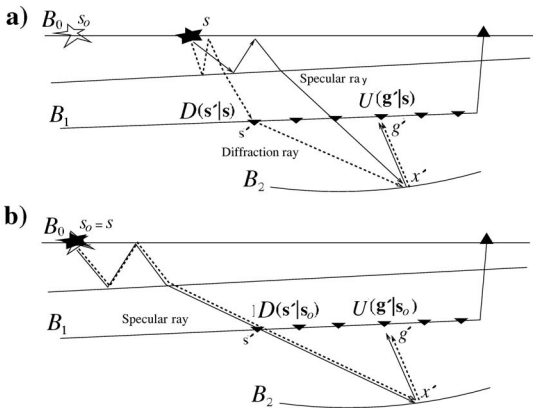

Figure 5. For fixed $\mathbf{s}'$ and $\mathbf{x}'$ positions, the traveltime difference between the solid pegleg specular and dashed pegleg diffraction rays is minimized when the solid star at $\mathbf{s}$ coincides with the open star at $\mathbf{s}_o$. This traveltime difference is nonzero in (a) but zero in (b).

$$\phi(\mathbf{g}',\mathbf{s}',\mathbf{s}) = e^{i\omega(\tau^{\text{peg}}_{g'x's} - \tau^{\text{peg}}_{ss'})}. \tag{26}$$

After summation over all source points $\mathbf{s}$, the traveltime of the downgoing pegleg recorded at $\mathbf{s}'$ will cancel part of the downgoing portion of the pegleg reflection traveltime recorded at $\mathbf{g}'$ under the stationary-phase approximation (see Figure 5b). Thus, the traveltime of the upgoing pegleg reflection transforms into that of a quasi-primary reflection excited by a secondary source at $\mathbf{s}'$ along the well and recorded at $\mathbf{g}'$.

CONCLUSIONS

We have reviewed the theory underlying both model-based and correlation-based redatuming methods. The natural methods (daylight imaging, interferometric imaging, reverse-time acoustics, virtual-source imaging) are superior to the model-based methods in that they do not require a velocity model and they eliminate statics at either the source and/or receiver locations. They can be used to redatum surface data to other datum levels. All natural redatuming methods can be described as summing weighted correlations of the traces for all of the source (and sometimes receiver) positions. These methods differ from one another by their choice of weights. In the frequency domain, we have the following (correlation weight, redatum method) pairs: (1, daylight imaging), (inverse source wavelet, interferometry), (inverse trace, virtual source), (Hessian inverse, least-squares interferometry), and (1, RTA). Least-squares interferometry and virtual-source imaging methods are potentially the most powerful because they account for the limited aperture and discrete sampling of the source and recording arrays. On the other hand, the interferometric imaging strategy is more flexible in that it can precisely target selected events for imaging, leading to a variety of applications such as redatuming methods for CDP reflections, converted waves, transmission waves, and pegleg multiples.

There are two main limitations of interferometric imaging methods for surface CDP data. First, the reference reflections must be identified and windowed. These windowed reference events can be correlated with either the traces or their picked traveltimes, which usually involves time-consuming user interaction. Well logs should be used to reduce misinterpretation of a multiple as a primary reference reflection. However, a potential benefit of entire-trace interferometric datuming is the potential to automatically account for near-surface multipathing arrivals that pass through the new datum level. Second, a rough estimate of the reference reflector's shape should be known to estimate the correct one-way traveltime from the two-way reference reflection time. The estimate of the reference reflector's shape can be made from the migration section.

A spin-off of interferometric wavefield imaging is the development of Fermat's interferometric principles for redatuming traveltimes associated with direct waves (transmission tomography), reflection waves (reflection traveltime tomography), or multiple reflections (multiple reflection tomography). Interesting applications include transforming VSP data into crosswell data. Finally, crosscorrelation of data is not needed for redatuming by seminatural Green's functions. This procedure is no more expensive than Kirchhoff migration and could reduce artifacts in migration images at the extra expense of picking or windowing about selected events.

All of these data-based redatuming methods enjoyed an independent genesis, yet they share the same fundamental operation: crosscorrelation and summation over source and/or geophone positions. These methods can be considered as special cases of interferometric least-squares redatuming, where each case selects a different approximation to the inverse Hessian. With specular interferometry, no correlation is needed, but the redatuming condition is derived from the crosscorrelation equations.

ACKNOWLEDGMENTS

The authors thank Andrey Bakulin and Rodney Calvert for their valuable contribution in describing the virtual-source imaging method. Many of the phrases in that section were written by Calvert. We also thank the Utah Tomography and Modeling/Migration (UTAM) sponsors for their generous support of this project (listed on http://utam.gg.
utah.edu). Helmut Jakubowicz pointed out that migrating multiples and primaries can lead to superresolution imaging. This idea was reinforced several months later in 2002 by George Papanicolaou at University of Minnesota's Institute for Mathematics and its Applications. We thank Panos Kelamis for forcing us to think about data-dependent imaging algorithms and Yi Luo for coining the term *seminatural Green's function*. We also thank Yi Luo for invigorating the seminatural Green's function approach by being the first to apply it successfully to VSP field data. We are grateful to Kees Wapenaar for insightful comments and Andrew Curtis for pointing out the diagonalization of the normal equations operator for an array of sources with random phase correlations.

REFERENCES

Asakawa, E., and T. Matsuoka, 2002, Traveltime-based raytracing for multiples and converted waves: 64th Annual Conference, EAGE, Extended Abstracts, P102.

Bakulin, A., and R. Calvert, 2004, Virtual source: New method for imaging and 4D below complex overburden: 74th Annual International Meeting, SEG, Expanded Abstracts, 2477–2480.

Berryhill, J. R., 1979, Wave-equation datuming: Geophysics, **44**, 1329–1344.

——–, 1986, Submarine canyons — Velocity replacement by wave-equation datuming before stack: Geophysics, **51**, 1572–1579.

Bevc, D., 1995, Imaging under rugged topography and complex velocity structure: Ph.D. dissertation, Stanford University.

Beylkin, G., 1985, Imaging of discontinuities in the inverse scattering problem by inversion of a causal generalized Radon transform: Journal of Mathematical Physics, **26**, 99–108.

Bleistein, N., J. Cohen, and J. Stockwell, 2001, Mathematics of multidimensional seismic imaging, migration, and inversion: Springer-Verlag, New York, Inc.

Blomgren, P., G. Papanicolaou, and H. Zhao, 2000, Super-resolution in time-reversal acoustics: Journal of the Acoustical Society of America, **108**, 230–248.
Bolte, J., and D. Verschuur, 2001, Velocity independent CFP redatuming: A strategy for subsalt imaging: 71st Annual International Meeting, SEG, 901–904.
Calvert, R. W., A. Bakulin, and T. C. Jones, 2004, Virtual sources, a new way to remove overburden problems: 66th Annual Conference, EAGE, Extended Abstracts, P234.
Claerbout, J., 1992, Earth soundings analysis: Processing versus inversion: Blackwell Scientific Publications, Inc.
Derode, A., E. Larose, M. Tanter, J. de Rosny, A. Tourin, M. Campillo, and M. Fink, 2003, Recovering the Green's function from field-field correlations in an open scattering medium: Journal of the Acoustical Society of America, **113**, 2973–2976.
Draganov, D., C. P. A. Wapenaar, and J. Thorbecke, 2003, Synthesis of the reflection response from the transmission response in the presence of white noise sources: 65th Annual Conference, EAGE, Extended Abstracts, P218.
Elmore, W., and M. Heald, 1969, Physics of waves: Dover Publishing, Inc.
Fink, M., 1992, Time reversal of ultrasonic fields: Part I — Basic principles: IEEE Transactions on Ultrasonics, Ferroelectrics and Frequency Control, **39**, 555–566.
Hageman, L., and D. Young, 1981, Applied iterative methods: Academic Press Inc.
Hornby, B., J. Yu, J. A. Sharp, A. Ray, Y. Quist, and C. Regone, 2006, VSP: Beyond time-to-depth: The Leading Edge, **25**, 446–452.
Jiang, Z., J. Yu, G. T. Schuster, and B. Hornby, 2005, Migration of multiples: The Leading Edge, **24**, 315–318.
Kelamis, P., K. Erickson, D. Verschuur, and A. Berkhout, 2002, Velocity-independent redatuming: A new approach to the near-surface problem in land seismic data processing: The Leading Edge, **21**, 730–735.
Lobkis, O., and R. Weaver, 2001, On the emergence of the Green's function in the correlations of a diffuse field: Journal of the Acoustical Society of America, **110**, 3011–3017.
Marsden, D., 1993, Static corrections — A review, Part III: The Leading Edge, **12**, 210–216.
Prada, C., E. Kerbrat, D. Cassereau, and M. Fink, 2002, Time reversal techniques in ultrasonic nondestructive testing of scattering media: Inverse Problems, **18**, 1761–1773.
Reshef, M., S. Keydar, and E. Landa, 2003, Multiple prediction without prestack data: An efficient tool for interpretive processing: First Break, **21**, 29–37.
Rickett, J., and J. Claerbout, 1996, Passive seismic imaging applied to synthetic data: Stanford Exploration Project, **92**, 83–90.
———, 1999, Acoustic daylight imaging via spectral factorization: Helioseismology and reservoir monitoring: The Leading Edge, **18**, 957–960.
———, 2000, Calculation of the acoustic solar impulse response by multi-dimensional spectral factorization: Solar Physics, **192**, no. 1/2, 203–210.
Rothman, D., 1986, Automatic estimation of large residual statics corrections: Geophysics, **51**, 332–346.
Schneider, W. A., Jr., L. D. Phillip, and E. F. Paal, 1995, Wave-equation velocity replacement of the low-velocity layer for overthrust-belt data: Geophysics, **60**, 573–580.
Schuster, G. T., 2001, Seismic interferometric/daylight imaging: Tutorial: 63rd Annual Conference, EAGE, Extended Abstracts.
———, 2003, Migrating the most bounce out of multiples: 65th Annual Conference, EAGE, Extended Abstracts, P4.
Schuster, G. T., and J. Rickett, 2000, Daylight imaging in V(x,y,z) media: Utah Tomography and Modeling-Migration Project Midyear Report, accessed April 2006 ⟨http://utam.gg.utah.edu/report.html⟩.
———, 2005a, Fermat's interferometric principles for target-oriented tomography: Geophysics, **70**, U47–U50.
———, 2005b, Fermat's interferometric principle for multiple reflection tomography: Geophysical Research Letters, **32**, L12303.
Schuster, G. T., J. Yu, and J. Sheng, 2004a, Migration, tomography and datuming by seismic interferometry: Annual Meeting, American Geophysical Union, Abstracts, S32A-01.
Schuster, G. T., J. Yu, J. Sheng, and J. Rickett, 2004b, Interferometric/daylight seismic imaging: Geophysical Journal International, **157**, 838–852.
Sheng, J., 2001, Migration multiples and primaries in CDP data by crosscorrelogram migration: 71st Annual International Meeting, SEG, Expanded Abstracts, 1297–1300.
Snieder, R., 2004, Extracting the Green's function from the correlation of coda waves: A derivation based on stationary phase: Physical Review E, **69**, 046610.
Snieder, R., A. Gret, H. Douma, and J. Scales, 2002, Coda wave interferometry for estimating nonlinear behavior in seismic velocity: Science, **295**, 2253–2255.
Taner, M. T., D. E. Wagner, E. Baysal, and L. Lu, 1998, A unified method for 2-D and 3-D refraction statics: Geophysics, **63**, 260–274.
Wapenaar, C. P. A., J. Thorbecke, and D. Draganov, 2004, Relation between reflection and transmission responses of 3-D inhomogeneous media: Geophysical Journal International, **156**, 179–194.
Wapenaar, K., 2003, Synthesis of an inhomogeneous medium from its acoustic transmission response: Geophysics, **68**, 1756–1761.
———, 2004, Retrieving the elastodynamic Green's function of an arbitrary inhomogeneous medium by cross correlation: Physical Review Letters, **93**, 254301-1–254301-4.
Wapenaar, K., D. Dragonov, J. Thorbecke, and J. Fokkema, 2002, Theory of acoustic daylight imaging revisited: 72nd Annual International Meeting, SEG, Expanded Abstracts, 2269–2272.
Wapenaar, K., J. Fokkema, and R. Snieder, 2005, Retrieving the Green's function in an open system by cross-correlations: A comparison of approaches: Journal of the Acoustical Society of America, **118** 2783–2786.
Xiao, X., M. Zhou, and G. T. Schuster, 2006, Salt flank delineation by PS interferometric imaging: Geophysics, this issue.
Yilmaz, O., and D. Lucas, 1986, Prestack layer replacement: Geophysics, **51**, 1355–1369.
Yu, J., and G. T. Schuster, 2001, Crosscorrelogram migration of IVSPWD data: 71st Annual International Meeting, SEG, Expanded Abstracts, 456–459.
———, 2004, Enhancing illumination coverage of VSP data by cross-correlogram migration: 74th Annual International Meeting, SEG, Expanded Abstracts, 2501–2504.
Zhou, M., and G. T. Schuster, 2006, Comparison between reduced-time migration and interferometric migration: Geophysics, this issue.
Zhu, X., D. P. Sixta, and B. G. Angstman, 1992, Tomo-statics: Turning-ray tomography + static corrections: The Leading Edge, **11**, 15–23.